

Integral Fractional Ornstein-Uhlenbeck Process Model for Animal Movement

José Hermenegildo Ramírez González¹ and Ying Sun¹

December 18, 2023

Abstract

Modeling the trajectories of animals is challenging due to the complexity of their behaviors, the influence of unpredictable environmental factors, individual variability, and the lack of detailed data on their movements. Additionally, factors such as migration, hunting, reproduction, and social interactions add additional layers of complexity when attempting to accurately forecast their movements. In the literature, various models exist that aim to study animal telemetry, by modeling the velocity of the telemetry, the telemetry itself or both processes jointly through a Markovian process. In this work, we propose to model the velocity of each coordinate axis for animal telemetry data as a fractional Ornstein-Uhlenbeck (fOU) process. Then, the integral fOU process models position data in animal telemetry. Compared to traditional methods, the proposed model is flexible in modeling long-range memory. The Hurst parameter $H \in (0, 1)$ is a crucial parameter in integral fOU process, as it determines the degree of dependence or long-range memory. The integral fOU process is nonstationary process. In addition, a higher Hurst parameter ($H > 0.5$) indicates a stronger memory, leading to trajectories with transient trends, while a lower Hurst parameter ($H < 0.5$) implies a weaker memory, resulting in trajectories with recurring trends. When $H = 0.5$, the process reduces to a standard integral Ornstein-Uhlenbeck process. We develop a fast simulation algorithm of telemetry trajectories using an approach via finite-dimensional distributions. We also develop a maximum likelihood method for parameter estimation and its performance is examined by simulation studies. Finally, we present a telemetry application of Fin Whales that disperse over the Gulf of Mexico.

Some key words: Animal tracking, finite-dimensional distribution approximation, fractional Brownian motion, Gaussian process simulations, telemetry data, trajectory prediction.

Short title: Integral Fractional Ornstein-Uhlenbeck Models.

¹CEMSE Division, Statistics Program, King Abdullah University of Science and Technology, Thuwal 23955-6900, Saudi Arabia. E-mail: josehermenegildo.ramirezgonzalez@kaust.edu.sa; ying.sun@kaust.edu.sa

1 Introduction

Our interest in animal movements is driven by scientific inquiry and the need to inform decisions related to the management and conservation of natural resources. Leveraging telemetry data has yielded valuable insights, allowing us to investigate essential ecological hypotheses concerning space utilization such as the animal’s location, its journey, its preferred habitat, and more.

Population dynamics encompass processes like births, deaths, immigration, and emigration. The integration of cutting-edge tracking technology and advanced statistical models can significantly enhance our comprehension of these phenomena. One of the most relevant techniques for animal conservation is the study of telemetry using statistical models. The primary importance of studying animal telemetry through statistical models lies in gaining a nuanced understanding of animal behavior, movement patterns, and population dynamics. Statistical models applied to telemetry data enable researchers to uncover hidden patterns, relationships, and ecological insights that contribute to informed conservation, management, and ecological decision-making. This approach facilitates the extraction of valuable information from complex data sets, aiding in the interpretation of animal movements, habitat preferences, and responses to environmental changes. Ultimately, statistical models enhance our ability to make scientifically grounded predictions and guide effective strategies for wildlife conservation and resource management.

In this work, we employ a movement model based on animal telemetry velocity, building on previous methodologies (Johnson et al. (2008); Matthiopoulos (2017); Torney et al. (2021)). Gaussian processes (GPs) have been applied in these works to model animal movement velocity within hierarchical models. Specifically, the velocity is modeled through linear stochastic differential equations (SDE), which can be expressed as GPs with a suitable covariance structure (Sarkka et al. (2013)). Notably, all random walk movement models that can be formulated as linear SDEs are also equivalent to GPs (Matthiopoulos (2017); Torney et al. (2021)). Among the crucial models for

velocity telemetry, the correlated random walk (CRW) model for animal movement can be formulated in both discrete-time (McClintock and Michelot (2018)) and continuous-time (Gurarie et al. (2017)). In the continuous-time version, a correlated velocity model is employed, also known as an Ornstein-Uhlenbeck (Uhlenbeck and Ornstein (1930)) velocity model or integrated Ornstein-Uhlenbeck model. Given that our data is non-stationary, we aim to derive a non-stationary version of the correlated velocity model. Specifically, we seek to develop a covariance matrix that represents the correlation structure in positional observations of an animal undergoing an autocorrelated continuous-time random walk with varying parameters. Our starting point is therefore an assumed movement model for the animal that is a non-stationary Ornstein-Uhlenbeck velocity model described by the following equations:

$$d\mu(t) = v(t)dt \text{ and } dv(t) = -a(t)v(t)dt + b(t)dW(t),$$

where μ is the position of the animal, v is its velocity, $W(t)$ is a Brownian motion, $a(t)$ and $b(t)$ are time-varying coefficients. In the case of constant parameters ($a(t) = a$ and $b(t) = b$) the covariance function of the Ornstein-Uhlenbeck process is well-known (Gardiner (2009)) and is equivalent to the exponential covariance function, i.e.,

$$\text{cov}(v(t), v(s)) = \frac{b^2}{2a} \exp(-a|t - s|). \tag{1}$$

To relate the covariance of the velocity process to the covariance of the positions, we note that for a zero-mean position process and by Fubini's theorem

$$\text{cov}(\mu(t), \mu(s)) = \int_0^t \int_0^s \text{cov}(v(u), v(w)) du dw. \tag{2}$$

Torney et al. (2021) consider the Matérn covariance function in the equation (1) and they studied

the telemetry of the animals by means of the covariance function given in (2). However, existing models do not allow us to study long-range dependence. Incorporating long-range dependency in models is important for achieving a more accurate and realistic representation of the temporal dependencies, leading to improved forecasting and overall model performance. One way we can introduce long-range dependency is by introducing more general noise. In this work, we consider a more general noise, through a fractional Ornstein-Uhlenbeck (fOU) process (Cheridito et al. (2003)) to model the velocity of each trajectory. Specifically,

$$dv_H(t) = -\beta v_H(t) + \sigma dW_H(t) \text{ and } d\mu_H(t) = v_H(t)dt, \quad (3)$$

where v_H is a fOU process is a stochastic process that has important applications in various fields, including finance, physics, and ecology. It is an extension of the classical Ornstein-Uhlenbeck process and is characterized by distinct properties. Unlike the traditional Ornstein-Uhlenbeck process, which has short-term memory, fOU process exhibits memory effects over a longer time scale so called long-memory property. This implies that the past values of the process have a significant influence on future values. Similar to the classical Ornstein-Uhlenbeck process, a fOU process can be stationary, meaning its statistical properties remain constant over time. Stationarity simplifies process analysis. The Hurst parameter $H \in (0, 1)$ is a crucial parameter in fOU process, as it determines the degree of long-range dependence or memory. A higher Hurst parameter ($H > 0.5$) indicates stronger memory, while a lower Hurst parameter ($H < 0.5$) implies weaker memory. When $H = 0.5$, the process is reduced to a standard Ornstein-Uhlenbeck process. Similar to the classical Ornstein-Uhlenbeck process, the fOU process exhibits mean-reverting behavior. This means that the process tends to return to a central or equilibrium point over time. When the Hurst parameter $H < 0.5$, it indicates positive correlation and thus recurrent trajectories. When $H > 0.5$, trajectories are more transitory. Estimating model parameters of a fOU process is challenging. We

can find several references (Brouste and Iacus (2013); Hu et al. (2019); Tanaka (2015); Xiao et al. (2011)) for the estimation of those parameters and asymptotic laws but the asymptotic results require the derivative of the position process. However, telemetry data usually do not include the velocity associated with the trajectory, and telemetry data are typically sparse in time, so that numerical methods often fail to estimate the derivative accurately. Therefore, we resort to the finite-dimensional laws of the position process, and the estimation is carried out via likelihood.

The rest of the paper is organized as follows. In Section 2, we present the definitions of the velocity and position process for modelling animal movement, with some examples of simulated trajectories and we establish some theoretical results of the position process $\mu_H(t)$, such as the autoregressive property and the derivation of its finite-dimensional distributions. In Section 3 we conduct simulation studies including the process $\mu_H(t)$. In Section 4 we derive explicitly likelihood function to estimate the parameters associated with the position process. In Section 5 we examine the performance of the maximum likelihood estimators (MLEs). In Section 6 we show the detailed analysis of telemetry data of Fin Whales whose habitat is the Gulf of Mexico. Finally, in Section 7 we conclude with a general discussion of the model and methodology. All the code is available on GitHub:

https://github.com/joseramirezgonzalez/Integral_fractional_Brownian_motion

2 Integral Fractional Ornstein-Uhlenbeck Process

In this section, we first give the definition of the velocity and position process of animal movement. We will then provide some examples of trajectories to visualize features of the process. Finally, we develop the finite-dimensional distributions of the position process in order to estimate the parameters.

Let $(W_H(t))_{t \geq 0}$ be a fractional Brownian motion (fBm) can be represented by a centered Gaussian

process with a covariance function

$$c_H(s, t) := \frac{1}{2} \left(t^{2H} + s^{2H} - |t - s|^{2H} \right), \text{ where } H \in (0, 1) \text{ is a Hurst parameter.} \quad (4)$$

fBm was introduced in (Mandelbrot and Van Ness (1968)). They proved that fBm can be represented by an integral with respect to Brownian motion $W(s)$:

$$W_H(t) = C_H \int_0^t (t - s)^{H-\frac{1}{2}} dW(s). \quad (5)$$

Then, we can resort to stochastic calculus to conduct the study of diffusion on fBm. In particular, the fractional Ornstein-Uhlenbeck process (fOU) $v_H(t)$ is defined by the following SDE:

$$dv_H(t) = -\beta v_H(t) + \sigma dW_H(t), \text{ where } \beta, \sigma > 0 \text{ are constants.} \quad (6)$$

We propose to model the velocity of movement of the animals, $v_H(t)$ as a fOU, and the position of the movement is given by the integral of the velocity. That is:

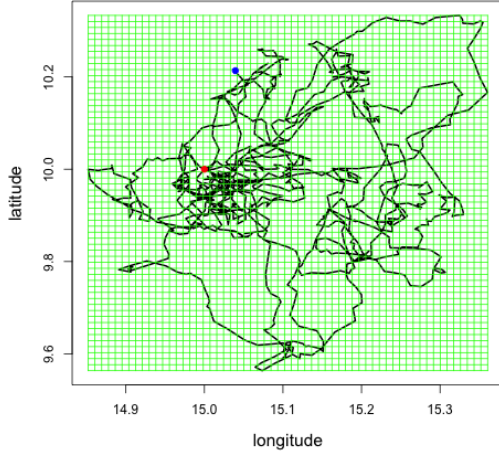
$$\mu_H(t) = \mu_H(0) + \int_0^t v_H(s) ds. \quad (7)$$

To study animal telemetry, we consider two independent position, $\mu_{H_1}(t)$ and $\mu_{H_2}(t)$ defined as in (7), each of which represents the position of the animal in longitude and latitude.

Figure 1 and Figure 2 show simulations of trajectories of the positioning process. Here, on each axis we consider an integral fOU process independent of each other. The trajectories are evaluated at times $0 = t_0 < t_1 < \dots < t_n = T$ and we consider $T = 20$, $n = 1000$, and $\Delta := t_i - t_{i-1} = \frac{1}{50}$ for $i = 1, \dots, n$. The parameters are $(\sigma_1 = \sqrt{3}, \beta_1 = 8.1, \mu_1(0) = 15, \sigma_2 = \sqrt{6}, \beta_2 = 2.7, \mu_2(0) = 10)$. Due to the correlation of the increments, we can see recurrent trajectories in the axis where the

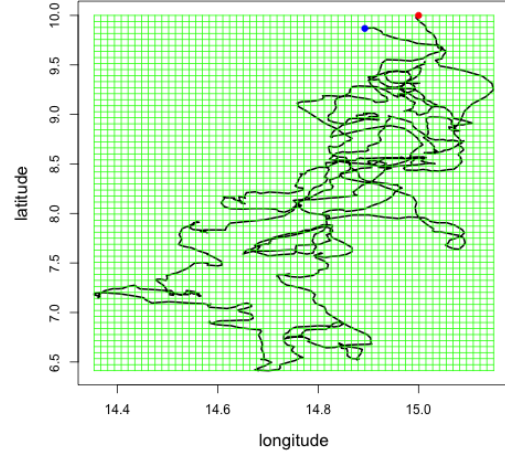
Hurst parameter $H \in (0, \frac{1}{2})$ and transient trajectories in the axis where the Hurst parameter $H \in (\frac{1}{2}, 1)$. Consequently, in Figure 1 (a), (b) and (c) and in Figure 2 (a), (b) and (c) we can see trajectories with recurrent and transitory trends respectively. Figure 1 (d) shows a trajectory when $(H_1 = H_2 = 0.5)$. This is the process used to model animal telemetry data in Johnson et al. (2008). Finally, Figure 2 (d) shows a trajectory that has a recurrence component and a transitory component in the axes. We can see recurring trend on the longitude axis and transient trend on the latitude axis.

Simulation Path Integral fOU process



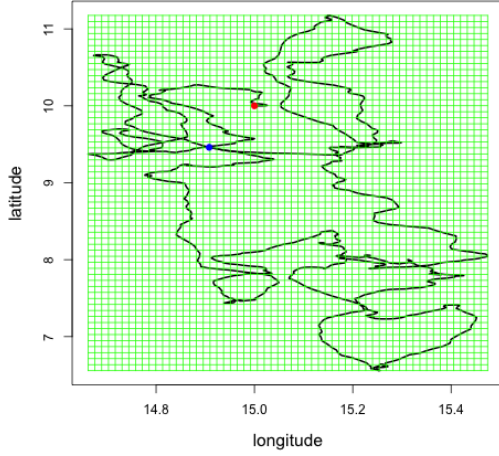
(a) ($H_1 = 0.04, H_2 = 0.02$)

Simulation Path Integral fOU process



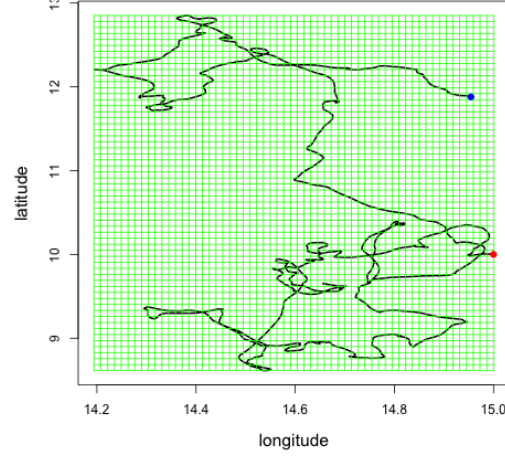
(b) ($H_1 = 0.22, H_2 = 0.18$)

Simulation Path Integral fOU process



(c) ($H_1 = 0.3, H_2 = 0.5$)

Simulation Path Integral fOU process



(d) ($H_1 = 0.5, H_2 = 0.5$)

Figure 1: Simulation of two independent integral fOU processes (one on each axis): In the simulations we consider $T = 20$ and $\Delta = \frac{1}{50}$ and the parameters are $(\sigma_1 = \sqrt{3}, \beta_1 = 8.1, \mu_1(0) = 15, \sigma_2 = \sqrt{6}, \beta_2 = 2.7, \mu_2(0) = 10)$.

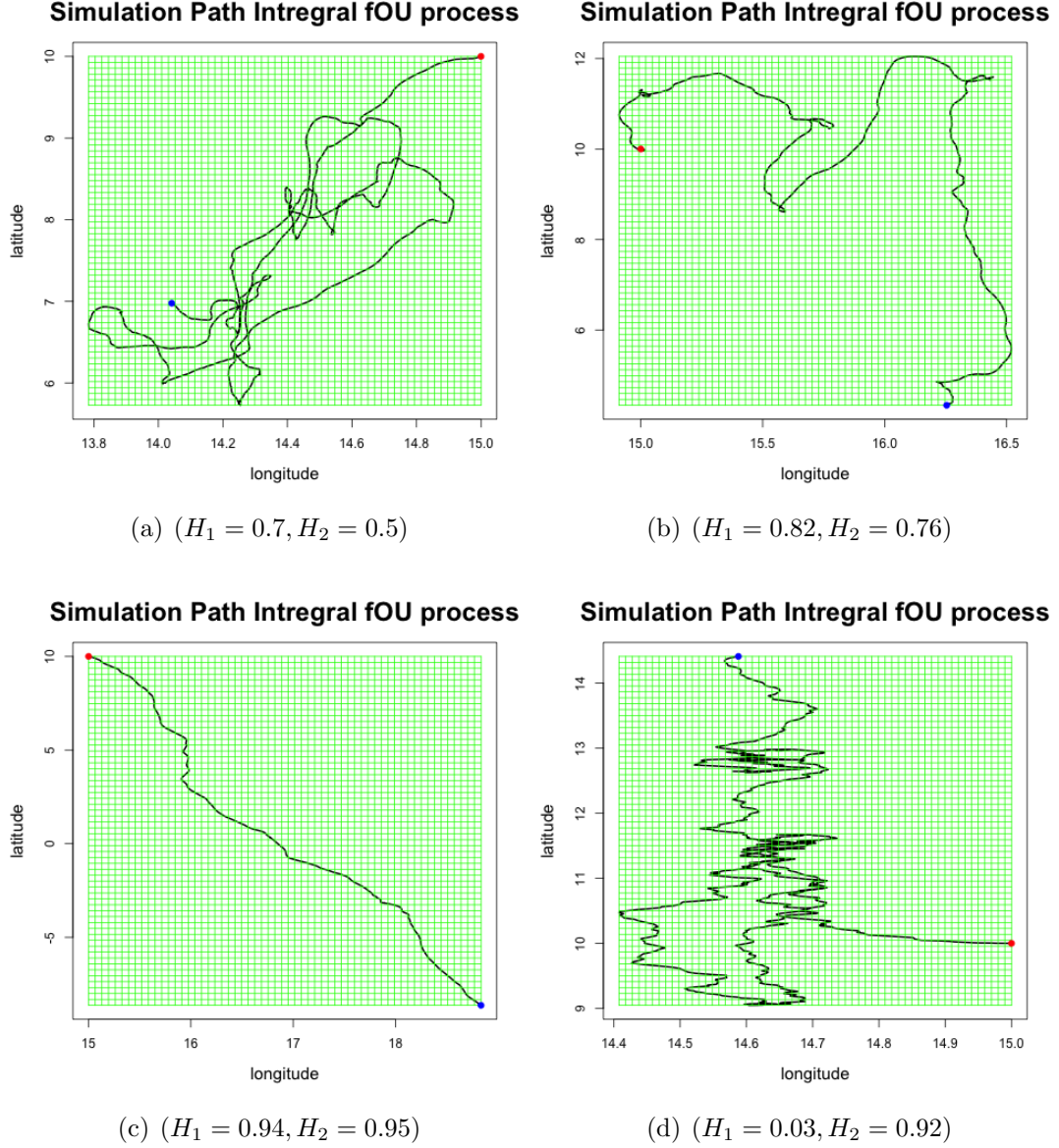


Figure 2: Simulation of two independent integral fOU processes (one on each axis): In the simulations we consider $T = 20$ and $\Delta = \frac{1}{50}$ and the parameters are $(\sigma_1 = \sqrt{3}, \beta_1 = 8.1, \mu_1(0) = 15, \sigma_2 = \sqrt{6}, \beta_2 = 2.7, \mu_2(0) = 10)$.

2.1 Theoretical Properties

In this section, we study certain properties of the processes defined in (6) and (7). In particular, the autoregressive property. In Proposition 2.1, we derive that velocity and position processes are Gaussian processes, and we derive the explicit forms of their mean and covariance functions.

We first establish the following results. The proof can be found in Appendix A.1.

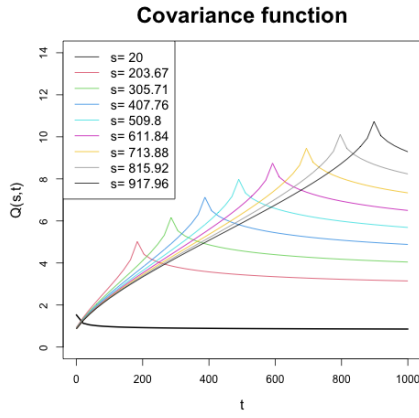
Proposition 2.1. $\mu_H(t)$ is a Gaussian process with mean

$$m(t) = \mu_H(0) + v_H(0) \left(\frac{1 - e^{-\beta t}}{\beta} \right) \quad (8)$$

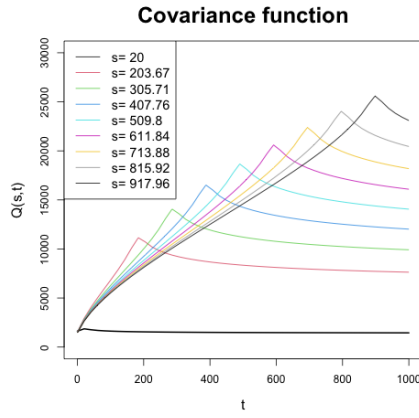
and covariance function

$$Q_{H,\beta,\sigma^2}(s, t) := \sigma^2 \int_0^t \int_0^s e^{-\beta v} \left(c_H(t - v, s - u) \right) e^{-\beta u} du dv \quad (9)$$

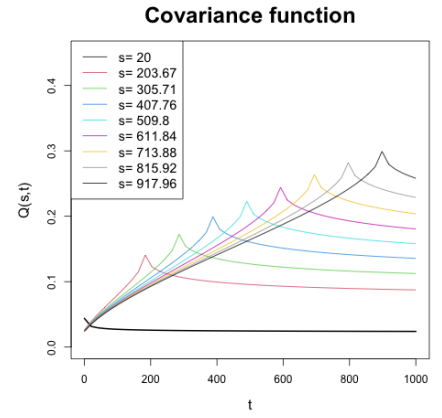
Figure 3 shows some examples of covariance functions given by the equation (9). In the fBm with covariance function c_H , we know that the Hurst parameters $H < 0.5$, indicates positive correlation between the increases and we have trajectories that result from recurrence, while when $H > 0.5$, we have trajectories that result from transient and when $H = 0.5$ the increases are not correlated. Consequently, for fixed s , when $H > 0.5$ ((g), (h) and (i)) we can see that the covariance function $Q_{H,\beta,\sigma^2}(s, \cdot)$ is increasing in $(0, \infty)$, when $H < 0.5$ ((a), (b) and (c)) $Q_{H,\beta,\sigma^2}(s, \cdot)$ is increasing from $(0, s)$ and decreasing from (s, ∞) . Finally, when $H = 0.5$ ((d), (e) and (f)) $Q_{H,\beta,\sigma^2}(s, \cdot)$ is increasing from $(0, s)$ and constant in (s, ∞)



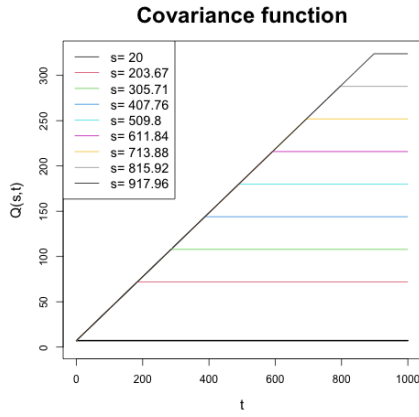
(a) ($H = 0.25, \sigma = 3, \beta = 5$)



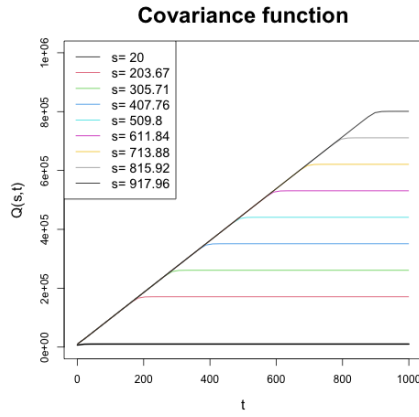
(b) ($H = 0.25, \sigma = 3, \beta = 0.1$)



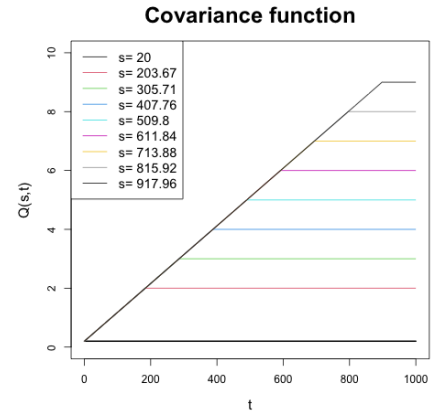
(c) ($H = 0.25, \sigma = 3, \beta = 30$)



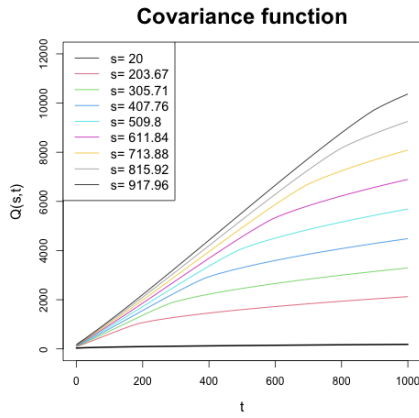
(d) ($H = 0.5, \sigma = 3, \beta = 5$)



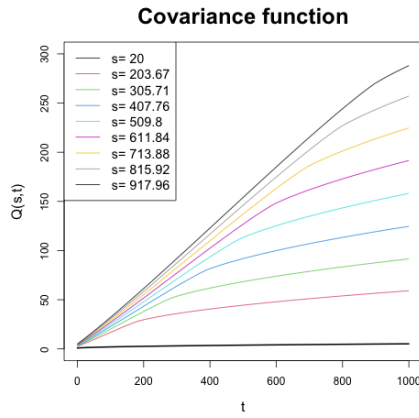
(e) ($H = 0.5, \sigma = 3, \beta = 0.1$)



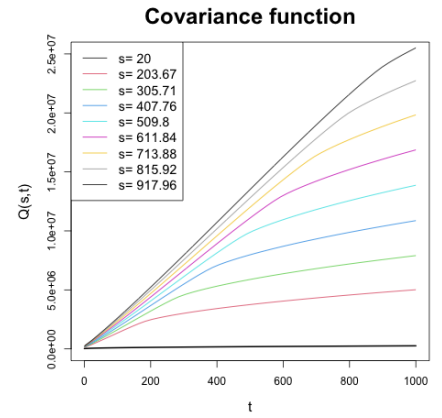
(f) ($H = 0.5, \sigma = 3, \beta = 30$)



(g) ($H = 0.75, \sigma = 3, \beta = 5$)



(h) ($H = 0.75, \sigma = 3, \beta = 0.1$)



(i) ($H = 0.75, \sigma = 3, \beta = 30$)

Figure 3: Examples of covariance functions associated with the position process.

In Proposition 2.2 we give autoregressive equation for the position and velocity vector. The proof can be found in Appendix A.1.

Proposition 2.2. *Let $\alpha_H(t) = (\mu_H(t), v_H(t))$. For any $\Delta > 0$ we have the equality*

$$\alpha(t + \Delta) = T\alpha(t) + \eta_t. \quad (10)$$

Here,

$$T = \begin{pmatrix} 1 & \frac{1-e^{-\beta\Delta}}{\beta} \\ 0 & e^{-\beta\Delta} \end{pmatrix};$$

and $\eta_{t,\Delta} \sim N((0, 0), \Sigma_{t,\Delta})$ where

$$\eta_{t,\Delta} = \left(\sigma \int_t^{t+\Delta} e^{\beta(s-(t+\Delta))} dW_H(s), \sigma \int_t^{t+\Delta} \frac{1 - e^{\beta(s-(t+\Delta))}}{\beta} dW_H(s) \right)^t.$$

and $\Sigma_{t,\Delta} := \text{cov}(\eta_{t,\Delta}, \eta_{t,\Delta})$

Remark 2.3. *Let $\Delta_i := t_{i+1} - t_i$, $i = 0, 1, \dots, n - 1$ and $\eta_i := \eta_{t_i, \Delta_i}$. When $H = \frac{1}{2}$ we will have that η_{t_i, Δ_i} and η_{t_j, Δ_j} are independent and the stochastic process $(\mu_H(t), v_H(t))$ is Markovian (see Johnson et al. (2008)). However, in the general case $H \neq \frac{1}{2}$ it is easy to see that η_{t_i, Δ_i} and η_{t_j, Δ_j} are correlated for $i \neq j$. In particular, to simulate finite-dimensional distributions of $\mu_H(t)$ we have to jointly simulate the random vectors $(\eta_{t_0, \Delta_0}, \dots, \eta_{t_{n-1}, \Delta_{n-1}})$. In Section 3 we give an efficient method of performing trajectory simulations of $\mu_H(t)$ by means of finite-dimensional distributions. Another consequence of such correlation is that that we cannot make use of the trajectory estimation technique given in (Johnson et al. (2008)) Kalman-Filter method.*

3 Simulation Studies

In this section we provide a method to simulate the finite-dimensional distributions of $\mu_H(t)$. First, we give a more efficient method for calculating the covariance function given in (9), and then make an approximation to the trajectories of $\mu_H(t)$ through their finite-dimensional distributions. In particular, given the continuity of the trajectories of $\mu_H(t)$ we show that the approximation via finite-dimensional distributions converges uniformly.

3.1 Fast simulation method

We proceed to simulate the finite-dimensional distributions of $\mu_H(t)$ and aim to approximate their trajectories utilizing the trajectories associated with $\mu_{H,n}(t)$ (see Proposition 3.4). Given the result of the Proposition 2.1 we can simulate a Gaussian vector with the covariance matrix:

$$Q_{t_i, t_j} := \sigma^2 \int_0^{t_i} \int_0^{t_j} e^{-\beta v} \left(C_H(t_i - v, t_j - u) \right) e^{-\beta u} du dv \quad (11)$$

for $0 = t_0 < t_1 < t_2 < \dots < t_n$ with $n \in \mathbb{N}$.

Remark 3.1. (i) If we have n distinct points, we need to calculate $\frac{n(n-1)}{2}$ integrals given in (11) to calculate the finite-dimensional distributions. This can be computationally inefficient.

(ii) For small values of t_i and large values of t_j or vice versa, there usually exist computational calculation errors. This can be avoided by integrating over intervals of the same order of length.

(iii) The calculation of finite-dimensional distributions allows us to estimate trajectories of $\mu_H(t)$, using maximum likelihood estimators.

Let $\Delta_i := t_{i+1} - t_i$, $i = 0, 1, \dots, n - 1$, and assume that $v_H(0) = 0$. Let

$$\begin{aligned}
\zeta_{t_i}^2 &:= \beta(1 - e^{-\beta\Delta_i})\mu_H(0) - \beta(\mu_H(t_i + \Delta_i) - e^{-\beta\Delta_i}\mu_H(t_i)) \\
&= -\sigma\beta \int_{t_i}^{t_i+\Delta_i} e^{\beta(s-(t_i+\Delta_i))} W_H(s) ds.
\end{aligned} \tag{12}$$

We define

$$y_i := \frac{\zeta_{t_i}^2}{\sigma\beta} = \int_{t_i}^{t_i+\Delta_i} e^{\beta(s-(t_i+\Delta_i))} W_H(s) ds \text{ for } i = 0, \dots, n-1$$

and $\mu_i := \mu_H(t_i)$ for $i = 1, \dots, n$ and we suppose that we know $\mu_0 := \mu_H(0)$.

In Proposition 3.2 we explicitly give the finite-dimensional distributions of $\mu_H(t)$. The proof can be found in Appendix A.2.

Proposition 3.2. *We have that*

$$(\mu_1, \dots, \mu_n)^t = (\mu_0, \dots, \mu_0)^t + \Sigma_{\beta, \sigma, (t_0, \dots, t_n)} \cdot (y_0, \dots, y_{n-1})^t \text{ where } (y_0, \dots, y_{n-1})^t \sim N(0, \Sigma_{H, \beta}). \tag{13}$$

Therefore, $(\mu_1, \dots, \mu_n)^t \sim N((\mu_0, \dots, \mu_0)^t, \Sigma_{\beta, \sigma, (t_0, \dots, t_n)} \Sigma_{H, \beta} \Sigma_{\beta, \sigma, (t_0, \dots, t_n)}^t)$, with

$$\Sigma_{\beta, \sigma, (t_0, \dots, t_n)} := \sigma \begin{pmatrix} 1 & 0 & 0 & 0 & \dots & 0 \\ e^{-\beta(t_2-t_1)} & 1 & 0 & 0 & \dots & 0 \\ e^{-\beta(t_3-t_1)} & e^{-\beta(t_3-t_2)} & 1 & 0 & \dots & \cdot \\ \cdot & \cdot & \cdot & \cdot & \dots & \cdot \\ \cdot & \cdot & \cdot & \cdot & \dots & \cdot \\ \cdot & \cdot & \cdot & \cdot & \dots & \cdot \\ e^{-\beta(t_n-t_1)} & e^{-\beta(t_n-t_2)} & e^{-\beta(t_n-t_3)} & e^{-\beta(t_n-t_4)} & \dots & 1 \end{pmatrix};$$

and

$$\Sigma_{H,\beta}(i+1, j+1) := \int_{t_j}^{t_j+\Delta_j} \int_{t_i}^{t_i+\Delta_i} e^{\beta(u-(t_i+\Delta_i))} e^{\beta(v-(t_j+\Delta_j))} c_H(u, v) dudv, \text{ for } i, j = 0, \dots, n-1.$$

Letting $\Delta_i = \Delta$, we have a way to perform simulations efficiently as shown below.

Remark 3.3. (*Fast simulations*) Being able to calculate the covariance function of $\mu_H(t)$ allows us to evaluate the likelihood of the trajectories to estimate the parameters. Then, we need to compute $\Sigma_{H,\beta}(i, j)$. In general case, we need to compute $\frac{n(n-1)}{2}$ double integral. But, if we assume that $\Delta_i = \Delta$. We only need compute n double integral and n simple integral. Suppose that $j \leq i$, it is easy to check that

$$\begin{aligned} \Sigma_{H,\beta}(i+1, j+1) &= \frac{1 - e^{-\beta\Delta}}{2\beta} \left(\int_0^\Delta e^{-\beta u} (t_j + \Delta - u)^{2H} du + \int_0^\Delta e^{-\beta u} (t_i + \Delta - u)^{2H} du \right) \\ &\quad - \frac{1}{2} \int_0^\Delta \int_0^\Delta e^{-\beta u} e^{-\beta v} |v - u + (i - j)\Delta|^{2H} dudv. \end{aligned}$$

Let

$$h(i) := \int_0^\Delta e^{-\beta u} ((i+1)\Delta - u)^{2H} du, \quad k(i) := \int_0^\Delta \int_0^\Delta e^{-\beta u} e^{-\beta v} |v - u + i\Delta|^{2H} dudv, \quad \text{for } i = 0, \dots, n-1. \quad (14)$$

Then, for $j \leq i$

$$\Sigma_{H,\beta}(j+1, i+1) = \Sigma_{H,\beta}(i+1, j+1) = \frac{1 - e^{-\beta\Delta}}{2\beta} \left(h(i) + h(j) \right) - \frac{1}{2} k(i - j) \quad (15)$$

and

$$\Sigma_{\beta,\sigma} := \sigma \begin{pmatrix} 1 & 0 & 0 & 0 & \dots & 0 \\ e^{-\beta\Delta} & 1 & 0 & 0 & \dots & 0 \\ e^{-2\beta\Delta} & e^{-\beta\Delta} & 1 & 0 & \dots & \cdot \\ \cdot & \cdot & \cdot & \cdot & \dots & \cdot \\ \cdot & \cdot & \cdot & \cdot & \dots & \cdot \\ \cdot & \cdot & \cdot & \cdot & \dots & \cdot \\ e^{-(n-1)\beta\Delta} & e^{-(n-2)\beta\Delta} & e^{-(n-3)\beta\Delta} & e^{-(n-4)\beta\Delta} & \dots & 1 \end{pmatrix}; \quad (16)$$

Therefore, based on equations (16), (15), (14) and (13), we can perform simulations of the finite-dimensional distributions of $\mu_H(t)$.

By means of finite-dimensional distributions of the process $\mu_H(t)$ we can uniformly approximate its trajectories. It is easy to prove that

Proposition 3.4. *Let $T > 0$ be fixed and $t_{i,n} = i\frac{T}{n}$ for $n \in \mathbb{N}$, $i = 0, \dots, n$. We define the process*

$$\begin{aligned} \mu_{H,n}(s) := & \sum_{i=0}^{n-2} 1_{[t_{i,n}, t_{i+1,n})}(s) \frac{T}{n} \left((t_{i+1,n} - s) \mu_H(t_{i,n}) + (s - t_{i,n}) \mu_H(t_{i+1,n}) \right) \\ & + 1_{[t_{n-1,n}, t_{n,n})}(s) \frac{T}{n} \left((t_{n,n} - s) \mu_H(t_{n-1,n}) + (s - t_{n-1,n}) \mu_H(t_{n,n}) \right), \quad \forall s \in [0, T]. \end{aligned} \quad (17)$$

Then, $\mu_H(t_{i,n}) = \mu_{H,n}(t_{i,n})$ for $i = 0, \dots, n$ and

$$\mu_{H,n}(t) \xrightarrow{n \rightarrow \infty} \mu_H(t) \text{ uniformly on } [0, T]$$

Given the position data (μ_0, \dots, μ_n) and the parameters by Proposition 3.5 we can by apply the theory of conditional Gaussian distributions for simulate values of $v_H(t)$ and vice versa, the proof can be found in Appendix A.2

Proposition 3.5. *We have recurring equations between velocity, position and noise. This is:*

$$v_H(t_i + \Delta_i) - e^{-\beta\Delta} v_H(t_i) = \zeta_{t_i}^1 + \zeta_{t_i}^2. \quad (18)$$

Here,

$$\zeta_{t_i}^1 := \sigma(W_H(t_i + \Delta_i) - e^{-\beta\Delta_i} W_H(t_i)) \quad (19)$$

Remark 3.6. To apply the theory of conditional Gaussian distributions, it is enough to calculate the covariance between $(\zeta_{t_j}^1, \zeta_{t_i}^1)$, $(\zeta_{t_j}^1, \zeta_{t_i}^2)$, $(\zeta_{t_j}^2, \zeta_{t_i}^1)$ and $(\zeta_{t_j}^2, \zeta_{t_i}^2)$. It is easy to check that:

$$\begin{aligned} \text{cov}\left(\zeta_{t_j}^1, \zeta_{t_i}^1\right) &= \sigma^2 \left[c_H(t_j + \Delta_j, t_i + \Delta_i) - e^{-\beta\Delta_i} C_H(t_j + \Delta_j, t_i) \right. \\ &\quad \left. - e^{-\beta\Delta_j} c_H(t_i + \Delta_i, t_j) + e^{-\beta(\Delta_i + \Delta_j)} c_H(t_i, t_j) \right] \end{aligned} \quad (20)$$

$$\text{cov}\left(\zeta_{t_j}^1, \zeta_{t_i}^2\right) = -\sigma^2 \beta \left[e^{-\beta\Delta_i} \int_{t_i}^{t_i + \Delta_i} e^{\beta(s-t_i)} c_H(t_j + \Delta_j, s) ds - e^{-\beta(\Delta_i + \Delta_j)} \int_{t_i}^{t_i + \Delta_i} e^{\beta(s-t_i)} c_H(t_j, s) ds \right] \quad (21)$$

$$\text{cov}\left(\zeta_{t_j}^2, \zeta_{t_i}^1\right) = -\sigma^2 \beta \left[e^{-\beta\Delta_j} \int_{t_j}^{t_j + \Delta_j} e^{\beta(s-t_j)} c_H(t_i + \Delta_i, s) ds - e^{-\beta(\Delta_i + \Delta_j)} \int_{t_j}^{t_j + \Delta_j} e^{\beta(s-t_j)} c_H(t_i, s) ds \right] \quad (22)$$

$$\text{cov}\left(\zeta_{t_j}^2, \zeta_{t_i}^2\right) = \sigma^2 \beta^2 e^{-\beta(\Delta_i + \Delta_j)} \int_{t_j}^{t_j + \Delta_j} \int_{t_i}^{t_i + \Delta_i} e^{\beta(v-t_j)} e^{\beta(u-t_i)} c_H(u, v) du dv \quad (23)$$

To perform simulations of finite-dimensional distributions, we can also use the following alternatives.

Remark 3.7. (*Design different data generating processes*)

We consider two alternative to simulate the trajectories of the process $\mu_H(t)$.

- Due to the equations (19), (12) and (18) we can use the Yuima R package software as in (Brouste and Iacus (2013)) to simulate the trajectories of $\mu_H(t)$. To do this, we jointly simulate $v_H(t_i = \Delta_i) - e^{-\beta\Delta}v_H(t_i)$ and $\sigma(W_H(t_i = \Delta_i) - e^{-\beta\Delta}W_H(t_i))$, and then apply equation (18).
- Approximation via the Riemann integral: use some software package to perform the simulation of $v_H(t)$ as in the previous point and subsequently perform the simulation of the trajectories of $\mu_H(t)$ by approximation of Riemann sums due to the equation (7).

3.2 Predictions

Given the Gaussianity of the process $\mu_H(t)$ we can use conditional laws to make future predictions of the trajectory of the animals.

$$y_i = \frac{1}{\sigma} \left((e^{-\beta\Delta_i} - 1)\mu_0 - e^{-\beta\Delta_i}\mu_i + \mu_{i+1} \right) \quad \text{for } i = 0, \dots, n-1. \quad (24)$$

We predict with $\Sigma_{H,\beta}$. Applying conditional distributions:

$$(y_{n+m-1}, \dots, y_n) | (y_{n-1}, \dots, y_0) \sim N \left(\Sigma_{(y_n, \dots, y_{n+m-1}), (y_n, \dots, y_{n+m-1})} \cdot \Sigma_{(y_0, \dots, y_{n-1}), (y_0, \dots, y_{n-1})}^{-1} \cdot (y_0, \dots, y_{n-1})^t, \right. \\ \left. \Sigma_{(y_n, \dots, y_{n+m-1}), (y_n, \dots, y_{n+m-1})} - \Sigma_{(y_n, \dots, y_{n+m-1}), (y_0, \dots, y_{n-1})} \cdot \Sigma_{(y_0, \dots, y_{n-1}), (y_0, \dots, y_{n-1})}^{-1} \cdot \Sigma_{(y_0, \dots, y_{n-1}), (y_n, \dots, y_{n+m-1})} \right) \quad (25)$$

Here,

$$\Sigma_{(y_n, \dots, y_{n+m-1}), (y_n, \dots, y_{n+m-1})} = \text{Cov} \left(\left(y_n, \dots, y_{n+m-1} \right), \left(y_n, \dots, y_{n+m-1} \right) \right)$$

$$\Sigma_{(y_n, \dots, y_{n+m-1}), (y_0, \dots, y_{n-1})} = \text{Cov} \left(\left(y_n, \dots, y_{n+m-1} \right), \left(y_0, \dots, y_{n-1} \right) \right)$$

and

$$\Sigma_{(y_0, \dots, y_{n-1}), (y_n, \dots, y_{n+m-1})} = \text{Cov} \left(\left(y_0, \dots, y_{n-1} \right), \left(y_n, \dots, y_{n+m-1} \right) \right) = \Sigma_{(y_n, \dots, y_{n+m-1}), (y_0, \dots, y_{n-1})}^t.$$

We calculate the predictions for μ_{i+1} by means of the equation

$$\mu_{i+1} = (1 - e^{-\beta \Delta_i}) \mu_0 + e^{-\beta \Delta_i} \mu_i + \sigma y_i \quad , \quad \text{for } i = n, \dots, n + (m - 1). \quad (26)$$

4 Inference

In the literature, such as (Brouste and Iacus (2013); Hu et al. (2019); Tanaka (2015); Xiao et al. (2011)), we can find theoretical results for various estimators of the parameters (σ, β, H) . However, these results require knowing the velocity trajectory or a specific sample of it. In practice, it is common that only sparsely sampled position trajectories are available, so we resort to maximum likelihood estimators to estimate the parameters.

First, we give some properties of the likelihood function associated with the finite-dimensional distributions of $\mu_H(t)$. Then, we describe a method to obtain maximum likelihood estimators.

From the equation (13) we know that $(\mu_1 - \mu_0, \dots, \mu_n - \mu_0) \sim N(0, \Sigma_{\beta, \sigma} \Sigma_{H, \beta} \Sigma_{\beta, \sigma}^t)$. Then, the log-likelihood function is given by:

$$\begin{aligned}
& \log \left(L \left((\sigma, \beta, h) \middle| (\mu_1 - \mu_0, \dots, \mu_n - \mu_0) \right) \right) \\
&= -\frac{1}{2\sigma^2} (\mu_1 - \mu_0, \dots, \mu_n - \mu_0)^t \left(\Sigma_{\beta,1} \Sigma_{H,\beta} \Sigma_{\beta,1}^t \right)^{-1} (\mu_1 - \mu_0, \dots, \mu_n - \mu_0) \\
&\quad - \frac{n}{2} \log(2\pi) - n \log(\sigma) - \frac{1}{2} \log(|\Sigma_{\beta,1} \Sigma_{H,\beta} \Sigma_{\beta,1}^t|)
\end{aligned} \tag{27}$$

Differentiating with respect to σ ,

$$\begin{aligned}
& \frac{\partial \log \left(L \left((\sigma, \beta, h) \middle| (\mu_1 - \mu_0, \dots, \mu_n - \mu_0) \right) \right)}{\partial \sigma} \\
&= \frac{1}{\sigma^3} (\mu_1 - \mu_0, \dots, \mu_n - \mu_0)^t \left(\Sigma_{\beta,1} \Sigma_{H,\beta} \Sigma_{\beta,1}^t \right)^{-1} (\mu_1 - \mu_0, \dots, \mu_n - \mu_0) - \frac{n}{\sigma}
\end{aligned} \tag{28}$$

We can see that it has a unique local maximum at $(0, \infty)$ and this is given by:

$$\hat{\sigma}(\beta, H) = \sqrt{\frac{\left(\Sigma_{\beta,1}^{-1} (\mu_1 - \mu_0, \dots, \mu_n - \mu_0) \right)^t \Sigma_{H,\beta}^{-1} \Sigma_{\beta,1}^{-1} (\mu_1 - \mu_0, \dots, \mu_n - \mu_0)}{n}} \tag{29}$$

Let's consider the profile log-likelihood function of (β, h) which is given by:

$$\begin{aligned}
\log \left(L_p \left((\beta, H) \middle| (\mu_1 - \mu_0, \dots, \mu_n - \mu_0) \right) \right) &= -\frac{n}{2} (1 + \log(2\pi)) - n \log(\hat{\sigma}(\beta, H)) - \frac{1}{2} \log(|\Sigma_{\beta,1} \Sigma_{H,\beta} \Sigma_{\beta,1}^t|) \\
&= -\frac{n}{2} (1 + \log(2\pi)) - \frac{1}{2} \log(|\Sigma_{\beta, \hat{\sigma}(\beta, H)} \Sigma_{H,\beta} \Sigma_{\beta, \hat{\sigma}(\beta, H)}^t|)
\end{aligned} \tag{30}$$

When the process is observed at different time scales, we now show the MLEs are scale-invariant in Proposition 4.1. Considering the amplitude time scale Δ , i.e., $t_i = i\Delta$. We will use the notation

$\Sigma_{\beta,1,\Delta}$, $\Sigma_{H,\beta,\Delta}$ and $\hat{\sigma}_\Delta(\beta, H)$ to indicate the Δ scale. The profile log-likelihood is defined as

$$f_\Delta(\beta, H) := -n \log(\hat{\sigma}_\Delta(\beta, H)) - \frac{1}{2} \log(|\Sigma_{\beta,1,\Delta} \Sigma_{H,\beta,\Delta} \Sigma_{\beta,1,\Delta}^t|)$$

The following results indicate that we can estimate the parameters independently of the scale. The proof is in Appendix A.3.

Proposition 4.1. *Let Δ_1 and Δ_2 be two scales. Then,*

(i)

$$f_{\Delta_2}(\beta, H) = f_{\Delta_1}\left(\frac{\beta \Delta_2}{\Delta_1}, H\right) \quad (31)$$

(ii) Suppose that $(\hat{\beta}, \hat{H}) \in (0, \infty) \times (0, 1)$ is the MLEs in Δ_1 scale. Then, $(\frac{\hat{\beta} \Delta_1}{\Delta_2}, \hat{H})$ is the MLEs in Δ_2 scale.

We can use the `optim` function of R software and the "L-BFGS-B" method to optimize the log-likelihood function like Section 5.1 or Section 5.2.

5 Numerical Studies

5.1 Estimation and Predictions

We perform a simulation with the following parameters: $T = 10$, $\Delta = \frac{1}{20}$, $\mu_1(0) = 15$, $\mu_2(0) = 10$, $(\sigma_1 = \sqrt{3}, \beta_1 = 12, H_1 = 0.56)$ and $(\sigma_2 = \sqrt{7}, \beta_2 = 6, H_2 = 0.75)$. By Proposition 4.1 we can consider $\Delta = 1$ for the estimate. Well, we will assume that we do not know the original scale of the data. Then, $T = n = 200$, we obtain the estimators $(\hat{\sigma}_1 = 1.0096892, \hat{\beta}_1 = 0.4649024, \hat{H}_1 = 0.4428731)$ and $(\hat{\sigma}_2 = 1.4782886, \hat{\beta}_2 = 0.1485762, \hat{H}_2 = 0.6350852)$. In Figure 4 shows profile likelihood of (β_1, H_1) (longitude) and (β_2, H_2) (latitude). Considering the original scale $\Delta = \frac{1}{20}$. We will have $T = 10$, $n = 200$ and the estimators are: $(\hat{\sigma}_1 = 1.2448453, \hat{\beta}_1 = 9.2980490, \hat{H}_1 = 0.4528731)$ and $(\hat{\sigma}_2 = 2.789843, \hat{\beta}_2 = 2.971524, \hat{H}_2 = 0.6350852)$.

The profile likelihood (β, H) function has a single global maximum.

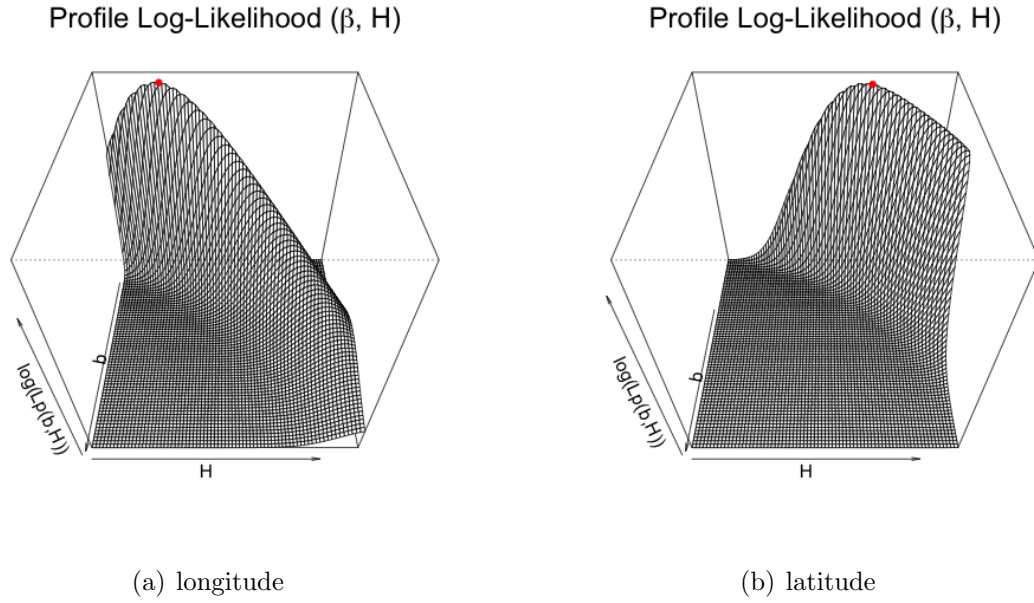


Figure 4: Profile Likelihood (β, H) for longitude and latitude.

Using the estimated parameters and the equations (24), (25) and (26) we can make trajectory predictions in the following n steps. Figure 5 shows the prediction of the next 10 steps. 100 simulations were carried out (red lines) and the average prediction (gray line) was considered for the prediction.

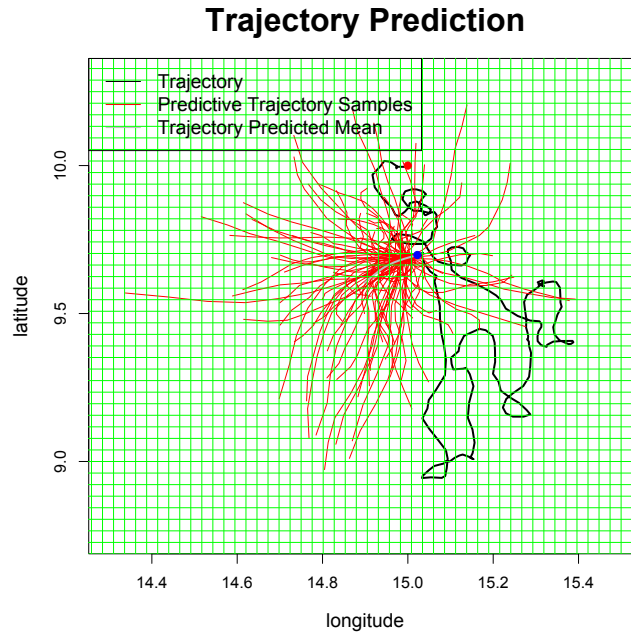


Figure 5: Trajectory Predictions

5.2 Simulation studies with respect to Δ .

In this section, we perform an analysis of simulations in order to show empirically that we have the consistency of the maximum likelihood estimators. Here, we consider $\mu_H(0) = 10$, $(\sigma = 2, \beta = 3, H = 0.1, 0.2, \dots, 0.9)$, $\Delta = 1/10, 1/20, \dots, 1/50$ and $T = 10$. In Figure 6, Figure 7 and Figure 8 we can empirically see the consistency of the MLEs. The more data we add to the likelihood function, the MLEs have a smaller mean square error.

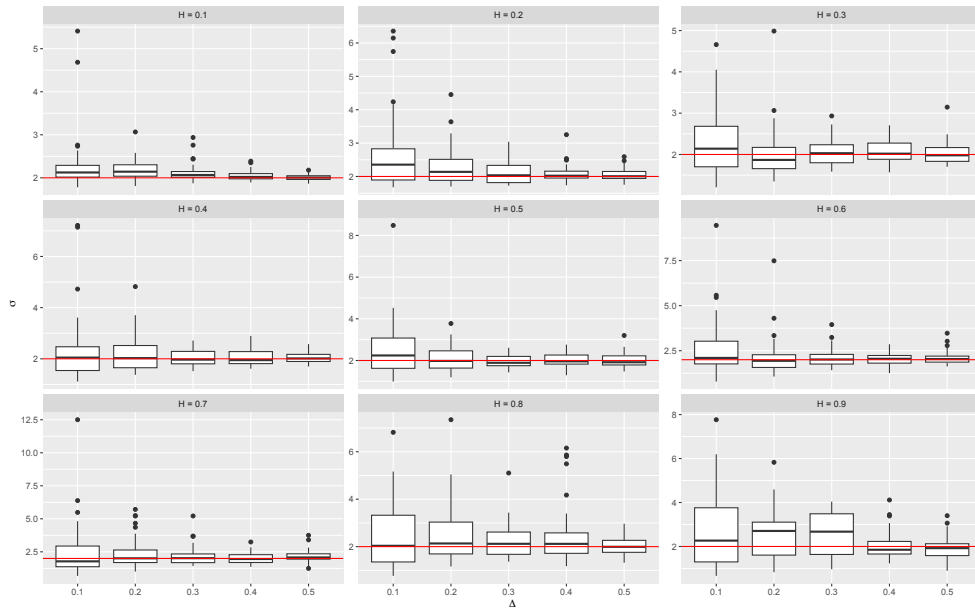


Figure 6: Represents the maximum likelihood estimator of σ with $\sigma = 2$, $\beta = 3$, $H = 0.1, 0.2, \dots, 0.9$ and $\Delta = 1/10, 1/20, \dots, 1/50$.

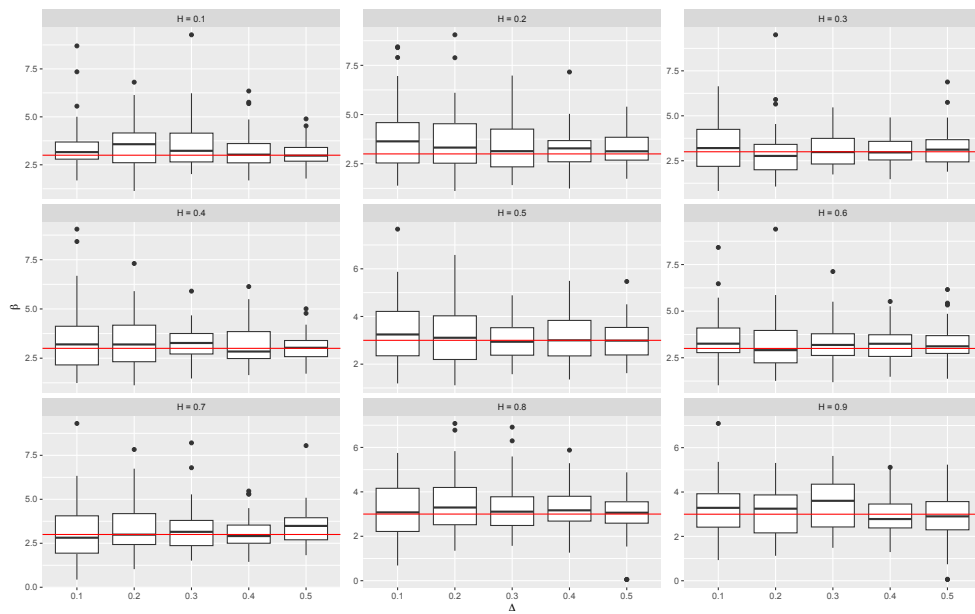


Figure 7: Represents the maximum likelihood estimator of β with $\sigma = 2$, $\beta = 3$, $H = 0.1, 0.2, \dots, 0.9$ and $\Delta = 1/10, 1/20, \dots, 1/50$.

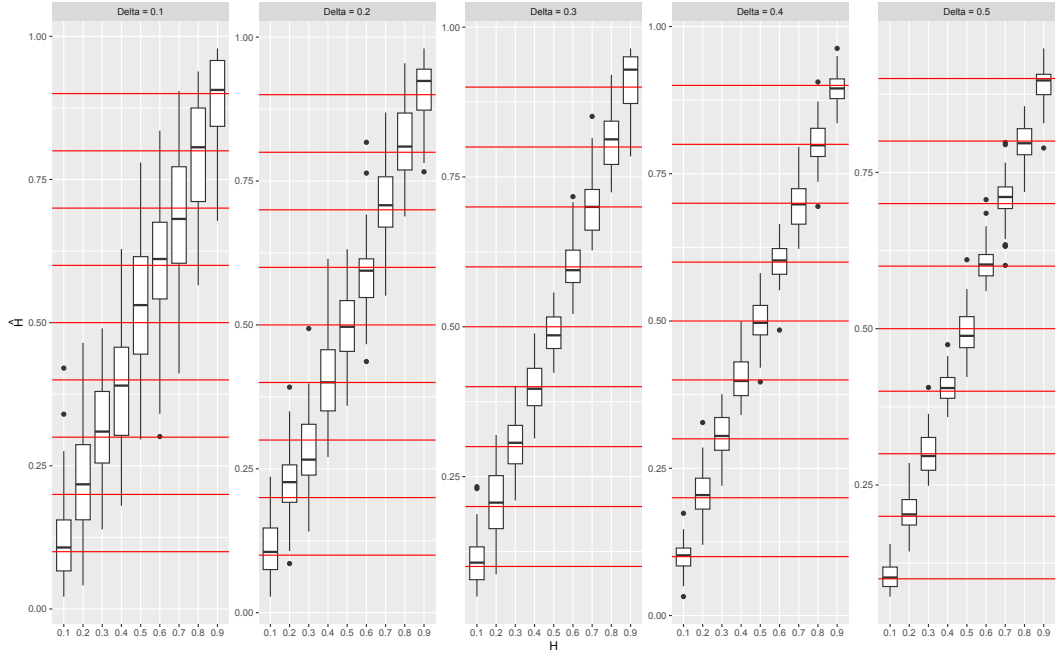


Figure 8: Represents the maximum likelihood estimator of H with $\sigma = 2$ $\beta = 3$ and $\Delta = 1/10, 1/20, \dots, 1/50$.

6 Application to Fin Whale data

In this section, we use the animal telemetry model described in Section 2 to the telemetry data of whales moving over the Gulf of Mexico. We assume that the velocity of the trajectories follows a fOU process. In Jiménez López et al. (2019) details about the database. Here, we only have position and time data. Therefore, we will perform parameter inference as in Section 4. That is, by the maximum likelihood method on finite-dimensional distributions.

We have telemetry data regarding eight Fin Whales that move over the Gulf of Mexico. These data were collected between March and September 2001. With respect to the whale identified with the number #1 we have longitude and latitude data ranging from the dates 03/28/2001 to 07/21/2001 we have a total of 87 records and 59 different days recorded. We consider grouping the data by daily records and on days where we have more than one record we consider their gravest

as points of longitude and latitude.

To model the position of the whale we will assume that its velocity process follows a fOU process. Since we only have longitude and latitude data, we will estimate the parameters via maximum likelihood as described in Section 4. We consider the scale $\Delta = 1$. Figure 9 shows the graph of $\log \left(L_p \left((\beta, H) \middle| (\mu_1 - \mu_0, \dots, \mu_n - \mu_0) \right) \right)$ for the latitude and longitude data for the position process. We can see that it has a single maximum.

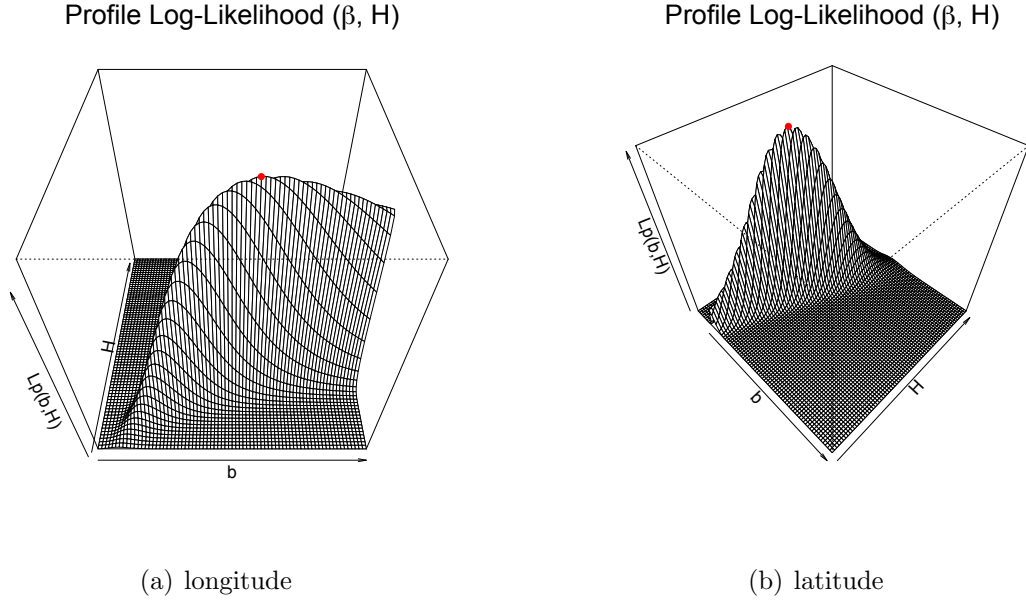


Figure 9: Profile Likelihood (β, h) for longitude and latitude.

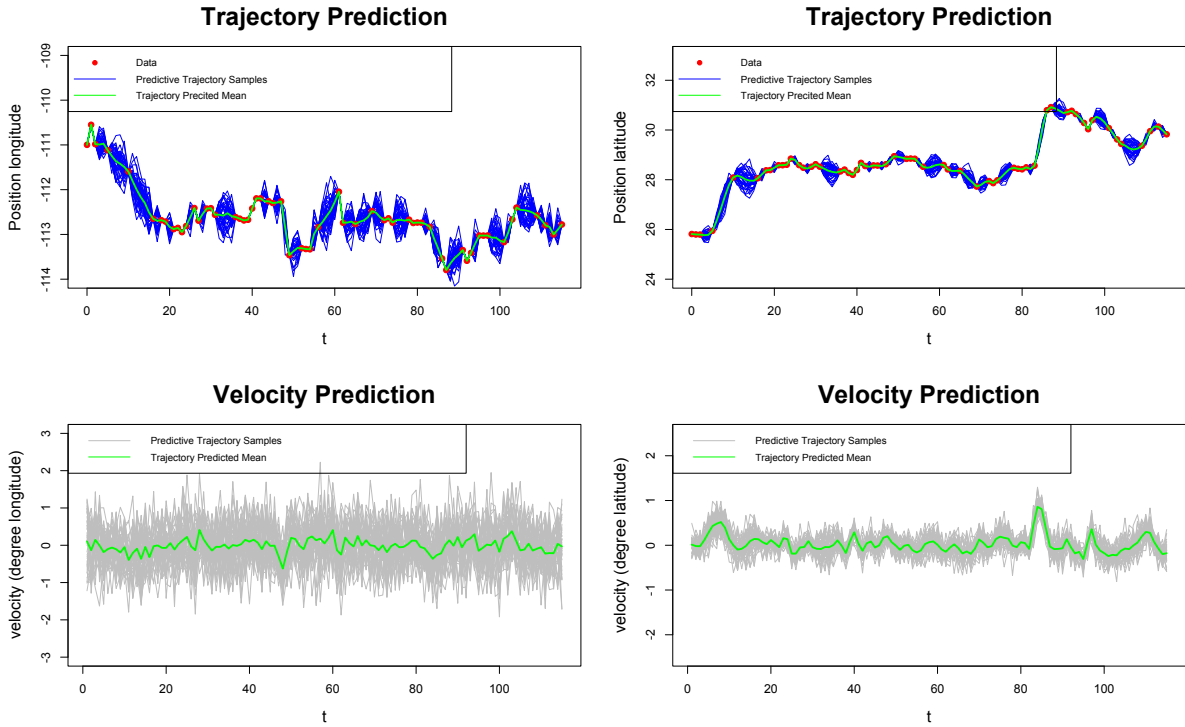
We obtain the estimators $(\hat{\sigma}_1 = 1.8060, \hat{\beta}_1 = 6.6453, \hat{H}_1 = 0.3968)$ and $(\hat{\sigma}_2 = 0.3793, \hat{\beta}_2 = 0.9291, \hat{H}_2 = 0.4431)$. Considering the Likelihood Ratio test for the null hypothesis $H = 0.5$. We have to:

$$-2 \log \left(\frac{L((1.8060, 6.6453, 0.5) | (\mu_{H_1}(t_0), \mu_{H_1}(t_1), \dots, \mu_{H_1}(t_n)))}{L((1.8060, 6.6453, 0.3968) | (\mu_{H_1}(t_0), \mu_{H_1}(t_1), \dots, \mu_{H_1}(t_n)))} \right) = 1.3531 < \chi_{0.95,1}^2 := 3.8414$$

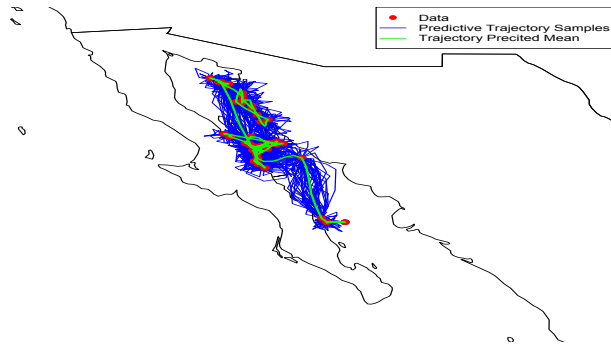
$$-2 \log \left(\frac{L((0.3793, 0.9291, 0.5)|(\mu_{H_1}(t_0), \mu_{H_1}(t_1), \dots, \mu_{H_1}(t_n)))}{L((0.3793, 0.9291, 0.4431)|(\mu_{H_1}(t_0), \mu_{H_1}(t_1), \dots, \mu_{H_1}(t_n)))} \right) = 0.4154 < \chi_{0.95,1}^2 = 3.8414$$

In this case the parameter $H = 0.5$ turns out to be a probable value given the position data (longitude and latitude).

In Figure 10 by conditional distribution of normal distribution and equations (19), (12) and (18), we can perform simulations of the velocity given the trajectory and maximum likelihood estimators. The blue lines represent simulations of trajectories considering the days when we do not have information.



(a) Trajectory Prediction and Velocity Prediction



(b) Trajectory Prediction

Figure 10: Estimation Trajectory for Fin Whale #1.

Regarding the whale identified with the number #3 we have longitude and latitude data ranging from the dates 03/31/2001 to 09/05/2001 we have a total of 217 records and 125 different days recorded. We consider grouping the data by daily records and on days where we have more than one record we consider their gravest as points of longitude and latitude.

We consider the scale $\Delta = 1$. Figure 11 shows the graph of $\log \left(L_p \left((\beta, H) \middle| (\mu_1 - \mu_0, \dots, \mu_n - \mu_0) \right) \right)$ for the latitude and longitude data for the position process. We obtain the estimators $(\hat{\sigma}_2 = 3.0218, \hat{\beta}_2 = 11.6463, \hat{H}_2 = 0.74713)$ for latitude and for longitude we select a β value where the likelihood does not have significant changes, since numerically it was not possible to find the MLE of β since the likelihood is flat $(\hat{\sigma}_1 = 2.0324, \hat{\beta}_1 = 7.811, \hat{H}_1 = 0.5581)$. For β greater than 7.811, the difference in likelihood is not significant ($< 10^{-3}$).

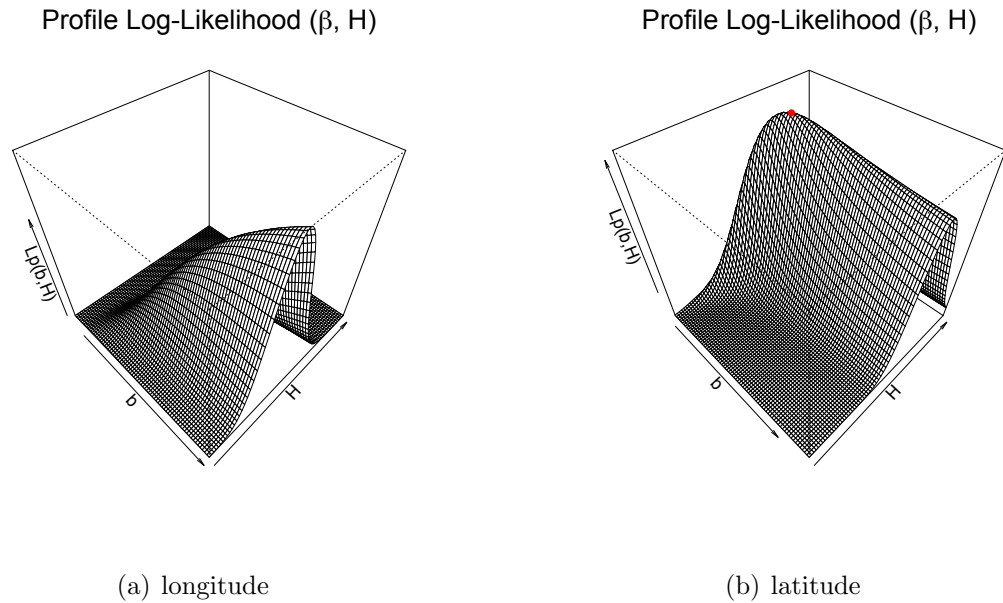


Figure 11: Profile Likelihood (β, h) for longitude and latitude.

In Figure 12 corresponds to the graph of (a) profile Likelihood β and (b) MLE of $\hat{\sigma}(\beta, \hat{H})$. In (b) we can see that if we fix H , the MLE of σ is increasing. Taking migration into account, we consider that it is appropriate to study the process locally in stationary areas. Well, globally, the model tries to explain migration by increasing the variance, but to do so through (b) we have to increase the value of β .

Considering the Likelihood Ratio test for the null hypothesis $H = 0.5$. For longitude we have

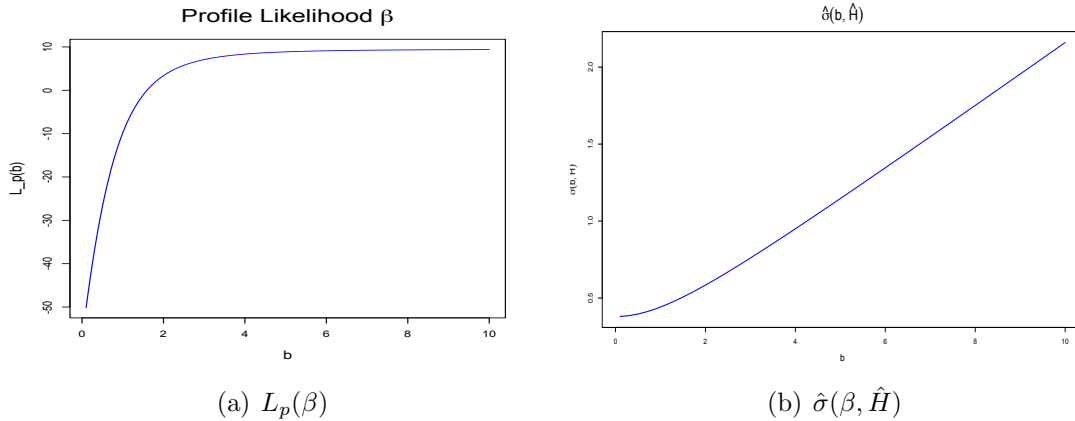
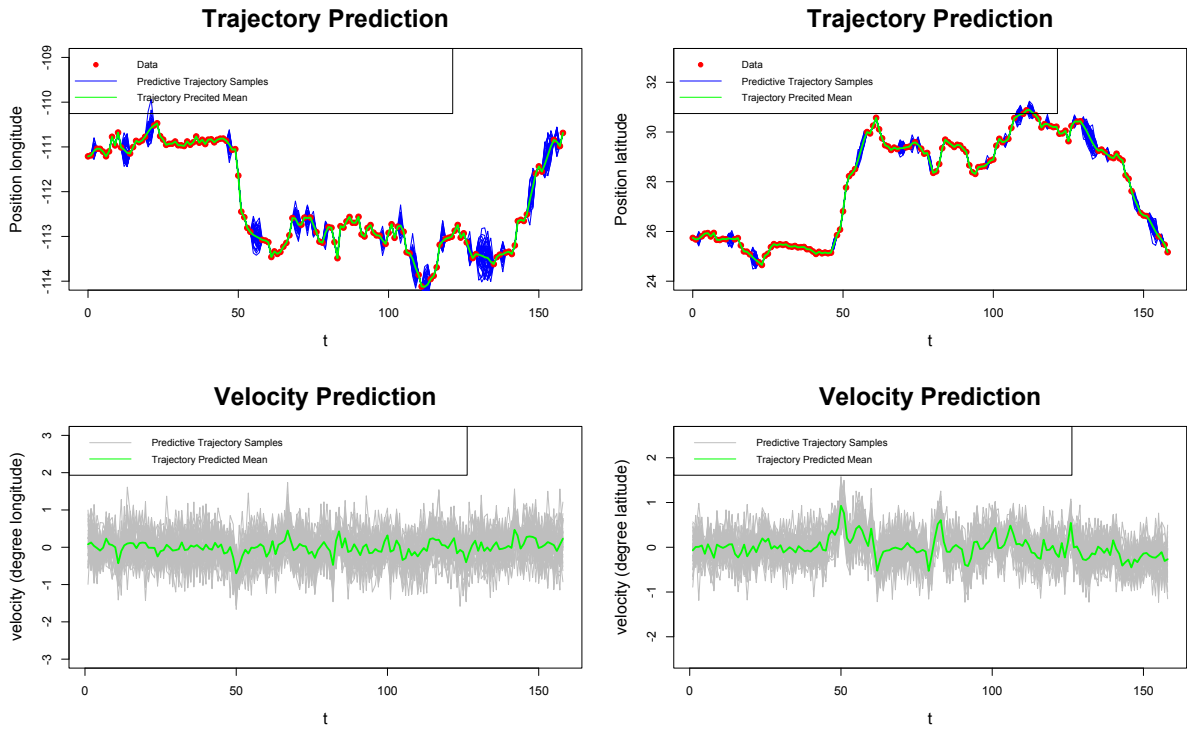
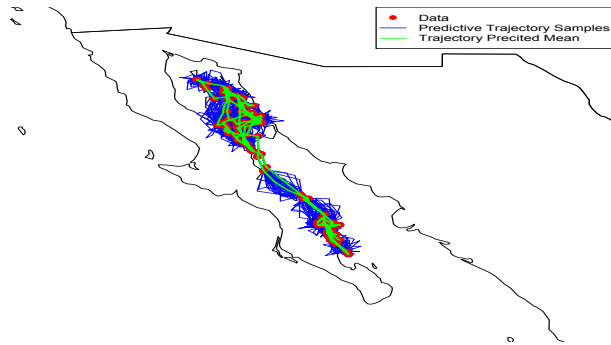


Figure 12: (a) Profile Likelihood β for Fin Whale #3 and (b) MLE of $\hat{\sigma}(\beta, \hat{H})$.

that the Likelihood Ratio is 0.4579 and for latitude the Likelihood Ratio is 22.24989. In this case the parameter $H = 0.5$ turns out to be a probable value given the position longitude data and for the latitude data we have to reject the null hypothesis $H = 0.5$, that is, the value of $H = 0.5$ does not turn out to be significant. In Figure 13 by conditional distribution of normal distribution and equations (19), (12) and (18), we can perform simulations of the velocity given the trajectory and maximum likelihood estimators. The blue lines represent simulations of trajectories considering the days when we do not have information.



(a) Trajectory Prediction and Velocity Prediction



(b) Trajectory Prediction

Figure 13: Estimation Trajectory for Fin Whale #3.

7 Discussion

In this work, it is assumed that the given movements in longitude and latitude are independent, which is not necessarily true. We have left that case for future work where cross-correlations that

respect the structure of the covariance function of each axis can be considered. For example, in (Lavancier et al. (2009); Amblard et al. (2013)) we can see an extension for $d - dimensional$ fractional Brownian motion with correlation structure. We can use this generalization to introduce correlation structures in the coordinate axes through the equation (9). Because the cross-correlation for the position could be calculated directly from the cross-correlation of a d-dimensional fractional Brownian motion with a correlation structure. Another interesting generalization would be to consider time-variation coefficients. That is, instead of considering β and σ . Consider functions $\beta(t)$ and $\sigma(t)$. However, we have left this for future work.

We have observed empirical consistency of the maximum likelihood estimators of the finite-dimensional distributions of $\mu_H(t)$. The theoretical consistency needs to be investigated.

Appendix A.1

Proof of Theoretical Properties.

Proof of Proposition 2.1

First, we will demonstrate that:

$$\mu_H(t) = \mu_H(0) + v_H(0) \left(\frac{1 - e^{-\beta t}}{\beta} \right) + \frac{\sigma}{\beta} \int_0^t (1 - e^{\beta(s-t)}) dW_H(s)$$

In fact, in (Cheridito et al. (2003)) they show that the equation (6) has a unit trajectory solution and its given by

$$v_H(t) = e^{-\beta t} \left(v_H(0) + \sigma \int_0^t e^{\beta s} dW_H(s) \right) \quad (32)$$

And in proposition A.1 they proved that

$$\int_0^t e^{\beta s} dW_H(s) = e^{\beta t} W_H(t) - \beta \int_0^t e^{\beta s} W_H(s) ds \quad (33)$$

Then, by equations (32) and (33) we have that:

$$\begin{aligned} \mu_H(t) &= \mu_H(0) + \int_0^t v_H(s) ds = \mu_H(0) + \int_0^t \left[e^{-\beta s} \left(v_H(0) + \sigma \int_0^s e^{\beta u} dW_H(u) \right) \right] ds \\ &= \mu_H(0) + v_H(0) \left(\frac{1 - e^{-\beta t}}{\beta} \right) + \sigma \int_0^t \int_0^s e^{\beta(u-s)} dW_H(u) ds \\ &= \mu_H(0) + v_H(0) \left(\frac{1 - e^{-\beta t}}{\beta} \right) + \frac{\sigma}{\beta} \int_0^t (1 - e^{\beta(s-t)}) dW_H(s) \end{aligned} \quad (34)$$

Finally, by equations (33) and (34) we have that

$$\begin{aligned}
& \text{cov} \left(\frac{\sigma}{\beta} \int_0^t (1 - e^{\beta(u-t)}) dW_H(u), \frac{\sigma}{\beta} \int_0^s (1 - e^{\beta(u-s)}) dW_H(u) \right) \\
&= \text{cov} \left(\sigma \int_0^t e^{\beta(u-t)} W_H(u) du, \sigma \int_0^s e^{\beta(u-s)} W_H(u) du \right) \\
&= \sigma^2 \int_0^t \int_0^s e^{\beta(v+u-t-s)} E \left(W_H(u) W_H(v) \right) dudv = \sigma^2 \int_0^t \int_0^s e^{-\beta v} \left(C_H(t-v, s-u) \right) e^{-\beta u} dudv
\end{aligned}$$

we conclude the proof. □

Now, we will demonstrate the autoregressive property of the velocity and position processes.

For the velocity process we have the next results:

Proposition 7.1. *For any $\Delta > 0$ we have*

$$v_H(t + \Delta) = e^{-\beta\Delta} v_H(t) + \sigma \int_t^{t+\Delta} e^{\beta(s-(t+\Delta))} dW_H(s). \quad (35)$$

Proof. By the equation (32) we have that:

$$\begin{aligned}
v_H(t + \Delta) &= e^{-\beta(t+\Delta)} v_H(0) + e^{-\beta(t+\Delta)} \sigma \int_0^t e^{\beta s} dW_H(s) + e^{-\beta(t+\Delta)} \sigma \int_t^{t+\Delta} e^{\beta s} dW_H(s) \\
&= e^{-\beta\Delta} v_H(t) + \sigma \int_t^{t+\Delta} e^{\beta(s-(t+\Delta))} dW_H(s)
\end{aligned} \quad (36)$$

We conclude the proof. □

For the position process we have the next results:

Proposition 7.2. *For any $\Delta > 0$, we have that*

$$\mu_H(t + \Delta) = \mu_H(t) + v_H(t) \left(\frac{1 - e^{-\beta\Delta}}{\beta} \right) + \frac{\sigma}{\beta} \int_t^{t+\Delta} \left(1 - e^{\beta(s-(t+\Delta))} \right) dW_H(s) \quad (37)$$

Proof. By equation (33) we have that

$$\begin{aligned} \int_0^t e^{-\beta u} \int_0^u e^{\beta s} dW_H(s) du &= \int_0^t \left[W_H(u) - \beta \int_0^u e^{\beta(s-u)} W_H(s) ds \right] du \\ &= \int_0^t W_H(u) du - \beta \int_0^t \int_s^t e^{\beta(s-u)} W_H(s) dud s \\ &= \int_0^t e^{\beta(s-t)} W_H(s) ds \end{aligned} \quad (38)$$

Random variable $\int_t^{t+\Delta} e^{\beta(s-(t+\Delta))} dW_H(s)$ satisfies the equality

$$\begin{aligned} \int_t^{t+\Delta} e^{\beta(s-(t+\Delta))} dW_H(s) &= e^{-\beta(t+\Delta)} \left[\int_0^{t+\Delta} e^{\beta s} dW_H(s) - \int_0^t e^{\beta s} dW_H(s) \right] \\ &= e^{-\beta(t+\Delta)} \left[e^{\beta(t+\Delta)} W_H(t + \Delta) - \beta \int_0^{t+\Delta} e^{\beta s} W_H(s) ds - \left(e^{\beta t} W_H(t) - \beta \int_0^t e^{\beta s} W_H(s) ds \right) \right] \\ &= W_H(t + \Delta) - e^{-\beta\Delta} W_H(t) - e^{-\beta(t+\Delta)} \beta \int_t^{t+\Delta} e^{\beta s} W_H(s) ds \end{aligned} \quad (39)$$

For any $\Delta > 0$, we have that

$$\int_0^{t+\Delta} e^{-\beta s} v_H(0) ds - \int_0^t e^{-\beta s} v_H(0) ds = v_H(0) e^{-\beta t} \left(\frac{1 - e^{-\beta\Delta}}{\beta} \right) \quad (40)$$

Therefore, by (33) and (39) it is easy to check that

$$\begin{aligned}
& \int_0^{t+\Delta} e^{-\beta u} \int_0^u e^{\beta s} dW_H(s) du - \int_0^t e^{-\beta u} \int_0^u e^{\beta s} dW_H(s) du \\
&= \frac{1 - e^{-\beta \Delta}}{\beta} e^{-\beta t} \int_0^t e^{\beta s} dW_H(s) + \int_t^{t+\Delta} \left(\frac{1 - e^{\beta(s-(t+\Delta))}}{\beta} \right) dW_H(s)
\end{aligned} \tag{41}$$

The proof follows from the equations (32), (40) and (41)

□

Proof of Proposition 2.2 It follows from the Propositions 7.1 and 7.2

□

Appendix A.2

Proof of Proposition 3.2: First, we will prove that

$$\mu_i = \mu_0 + \sigma \sum_{j=0}^{i-1} y_j e^{-\beta(t_i - t_{j+1})} \tag{42}$$

By equation (19) we have that:

$$-\beta \sigma y_i = \beta(1 - e^{-\beta \Delta_i}) \mu_0 - \beta(\mu_{i+1} - e^{-\beta \Delta_i} \mu_i) \quad i = 0, \dots, n-1 \tag{43}$$

In (43) put $i = 0$ we have that:

$$-\beta \sigma y_0 = \beta(1 - e^{-\beta \Delta_0}) \mu_0 - \beta(\mu_1 - e^{\beta \Delta_0} \mu_0) = \beta \mu_0 - \beta \mu_1$$

Then, $\mu_1 = \mu_0 + \sigma y_0$. We have the equation (42) with $i = 1$. We suppose that we have equation (42) for some $m \in \mathbb{N}$. We proof that we have equation (42) for $m + 1$. In fact,

$$\begin{aligned}
\mu_{m+1} &= (1 - e^{-\beta\Delta_m})\mu_0 + e^{-\beta\Delta_m}\mu_m + \sigma y_m \\
&= (1 - e^{-\beta\Delta_m})\mu_0 + e^{-\beta\Delta_m}\left(\mu_0 + \sigma \sum_{j=0}^{m-1} y_j e^{-\beta(t_m - t_{j+1})}\right) + \sigma y_m \\
&= \mu_0 + \sigma \sum_{j=0}^{m-1} y_j e^{-\beta(t_{m+1} - t_{j+1})} + \sigma y_m = \mu_0 + \sigma \sum_{j=0}^m y_j e^{-\beta(t_{m+1} - t_{j+1})}
\end{aligned}$$

Now, it is evident that

$$\text{cov}(y_j, y_i) = \int_{t_j}^{t_j + \Delta_j} \int_{t_i}^{t_i + \Delta_i} e^{\beta(u - (t_i + \Delta_i))} e^{\beta(v - (t_j + \Delta_j))} c_H(u, v) dudv := \Sigma_{H, \beta}(i+1, j+1), \text{ for } i, j = 0, \dots, n-1$$

From where we conclude the proof. □

Proof of Proposition 3.5: By the equation (38) we have that:

$$\mu_H(t + \Delta) = \mu_H(0) + v_H(0) \left(\frac{1 - e^{-\beta(t + \Delta)}}{\beta} \right) + \frac{\sigma}{\beta} \int_0^{t + \Delta} (1 - e^{\beta(s - (t + \Delta))}) dW_H(s)$$

and

$$e^{-\beta\Delta} \mu_H(t) = e^{-\beta\Delta} \mu_H(0) + v_H(0) \left(\frac{e^{-\beta\Delta} - e^{-\beta(t + \Delta)}}{\beta} \right) + \frac{\sigma}{\beta} \int_0^t \left(e^{-\beta\Delta} - e^{\beta(s - (t + \Delta))} \right) dW_H(s)$$

Therefore,

$$\begin{aligned}
\mu_H(t + \Delta) - e^{-\beta\Delta} \mu_H(t) &= (1 - e^{-\beta\Delta})\mu_H(0) + v_H(0) \left(\frac{1 - e^{-\beta\Delta}}{\beta} \right) \\
&\quad + \frac{\sigma}{\beta} (W_H(t + \Delta) - e^{-\beta\Delta} W_H(t)) - \frac{\sigma}{\beta} \int_t^{t + \Delta} e^{\beta(s - (t + \Delta))} dW_H(s)
\end{aligned} \tag{44}$$

Furthermore, by the equation (36)

$$\frac{1}{\beta} \left(v_H(t + \Delta) - e^{-\beta\Delta} v_H(t) \right) = \frac{\sigma}{\beta} \int_t^{t+\Delta} e^{\beta(s-(t+\Delta))} dW_H(s)$$

Finally, under the assumption $v_H(0) = 0$.

$$\begin{aligned} v_H(t + \Delta) - e^{-\beta\Delta} v_H(t) &= \beta(1 - e^{-\beta\Delta})\mu_H(0) + \sigma(W_H(t + \Delta) - e^{-\beta\Delta}W_H(t)) \\ &\quad - \beta(\mu_H(t + \Delta) - e^{-\beta\Delta}\mu_H(t)) \end{aligned} \quad (45)$$

Appendix A.3

Proof of Proposition 4.1: (i) Obviously $\Sigma_{\beta,1,\Delta_2} = \Sigma_{\frac{\beta\Delta_2}{\Delta_1},1,\Delta_1}$. Furthermore, by changing the variable $(u', v') = \frac{\Delta_1}{\Delta_2}(u, v)$ we have that

$$\begin{aligned} \int_0^{\Delta_2} \int_0^{\Delta_2} e^{-\beta u} c_H(\Delta_2(i+1) - u, \Delta_2(j+1) - v) e^{-\beta v} dudv \\ = \left(\frac{\Delta_2}{\Delta_1}\right)^{2+2H} \int_0^{\Delta_1} \int_0^{\Delta_1} e^{-\frac{\beta\Delta_2}{\Delta_1}u} c_H(\Delta_1(i+1) - u, \Delta_1(j+1) - v) e^{-\frac{\beta\Delta_2}{\Delta_1}v} dudv \end{aligned}$$

Then,

$$\Sigma_{H,\beta,\Delta_2} = \left(\frac{\Delta_2}{\Delta_1}\right)^{2+2H} \Sigma_{H,\frac{\beta\Delta_2}{\Delta_1},\Delta_1}$$

Therefore,

$$\begin{aligned} \hat{\sigma}_{\Delta_2}(\beta, H) &= \sqrt{\frac{(\mu_1 - \mu_0, \dots, \mu_n - \mu_0)^t (\Sigma_{\beta,1,\Delta_2} \Sigma_{H,\beta,\Delta_2} \Sigma_{\beta,1,\Delta_2}^t)^{-1} (\mu_1 - \mu_0, \dots, \mu_n - \mu_0)}{n}} \\ &= \left(\frac{\Delta_1}{\Delta_2}\right)^{1+H} \sqrt{\frac{(\mu_1 - \mu_0, \dots, \mu_n - \mu_0)^t (\Sigma_{\frac{\beta\Delta_2}{\Delta_1},1,\Delta_1} \Sigma_{H,\frac{\beta\Delta_2}{\Delta_1},\Delta_1} \Sigma_{\frac{\beta\Delta_2}{\Delta_1},1,\Delta_1}^t)^{-1} (\mu_1 - \mu_0, \dots, \mu_n - \mu_0)}{n}} \end{aligned}$$

Finally,

$$\begin{aligned} f_{\Delta_2}(\beta, H) &= -n(1 + H) \log\left(\frac{\Delta_1}{\Delta_2}\right) - n \log(\hat{\sigma}_{\Delta_1}\left(\frac{\beta\Delta_2}{\Delta_1}, H\right)) - n(1 + H) \log\left(\frac{\Delta_2}{\Delta_1}\right) \\ &\quad - \frac{1}{2} \log(|\Sigma_{\frac{\beta\Delta_2}{\Delta_1}, 1, \Delta_1} \Sigma_{H, \frac{\beta\Delta_2}{\Delta_1}, \Delta_1} \Sigma_{\frac{\beta\Delta_2}{\Delta_1}, 1, \Delta_1}|) \\ &= f_{\Delta_1}\left(\frac{\beta\Delta_2}{\Delta_1}, H\right) \end{aligned}$$

(ii) It is immediate of (i).

We conclude the proof.

□

References

- Amblard, P., Coeurjolly, J.-F., Lavancier, F., and Philippe, A. (2013). Basic properties of the Multivariate Fractional Brownian Motion. *Séminaires et Congrès- SMF*, 28:65–87.
- Brouste, A. and Iacus, S. M. (2013). Parameter estimation for the discretely observed fractional Ornstein–Uhlenbeck process and the Yuima R package. *Computational Statistics*, 28(4):1529–1547.
- Cheridito, P., Kawaguchi, H., and Maejima, M. (2003). Fractional Ornstein-Uhlenbeck processes. *Electronic Journal of Probability*, 8(none):1 – 14. Publisher: Institute of Mathematical Statistics and Bernoulli Society.
- Gardiner, C. (2009). *Stochastic methods: A handbook for the natural and social sciences*. Springer, Berlin., 4th ed. edition.
- Gurarie, E., Fleming, C. H., Fagan, W. F., Laidre, K. L., Hernández-Pliego, J., and Ovaskainen, O. (2017). Correlated velocity models as a fundamental unit of animal movement: synthesis and applications. *Movement Ecology*, 5(1):13.
- Hu, Y., Nualart, D., and Zhou, H. (2019). Parameter estimation for fractional Ornstein-Uhlenbeck processes of general Hurst parameter. *Statistical Inference for Stochastic Processes*, 22.
- Jiménez López, M. E., Palacios, D. M., Jaramillo Legorreta, A., Urbán R., J., and Mate, B. R. (2019). Fin whale movements in the Gulf of California, Mexico, from satellite telemetry. *PLOS ONE*, 14(1):e0209324. Publisher: Public Library of Science.
- Johnson, D. S., London, J. M., Lea, M.-A., and Durban, J. W. (2008). CONTINUOUS-TIME CORRELATED RANDOM WALK MODEL FOR ANIMAL TELEMETRY DATA. *Ecology*, 89(5):1208–1215. Publisher: John Wiley & Sons, Ltd.

- Lavancier, F., Philippe, A., and Surgailis, D. (2009). Covariance function of vector self-similar processes. *Statistics & Probability Letters*, 79(23):2415–2421.
- Mandelbrot, B. B. and Van Ness, J. W. (1968). Fractional Brownian Motions, Fractional Noises and Applications. *SIAM Review*, 10(4):422–437. Publisher: Society for Industrial and Applied Mathematics.
- Matthiopoulos, J. (2017). Animal Movement: Statistical Models for Telemetry Data by Hooten, Johnson, McClintock and Morales. *Journal of Agricultural, Biological and Environmental Statistics*, 22.
- McClintock, B. T. and Michelot, T. (2018). momentuHMM: R package for generalized hidden Markov models of animal movement. *Methods in Ecology and Evolution*, 9(6):1518–1530. Publisher: John Wiley & Sons, Ltd.
- Sarkka, S., Solin, A., and Hartikainen, J. (2013). Spatiotemporal learning via infinite-dimensional bayesian filtering and smoothing: A look at gaussian process regression through kalman filtering. *IEEE Signal Processing Magazine*, 30(4):51–61.
- Tanaka, K. (2015). Maximum likelihood estimation for the non-ergodic fractional Ornstein–Uhlenbeck process. *Statistical Inference for Stochastic Processes*, 18(3):315–332.
- Torney, C., Morales, J., and Husmeier, D. (2021). A hierarchical machine learning framework for the analysis of large scale animal movement data. *Movement Ecology*, 9.
- Uhlenbeck, G. E. and Ornstein, L. S. (1930). On the theory of the brownian motion. *Phys. Rev.*, 36:823–841.
- Xiao, W., Zhang, W., and Xu, W. (2011). Parameter estimation for fractional Ornstein–Uhlenbeck processes at discrete observation. *Applied Mathematical Modelling*, 35(9):4196–4207.